Journal of Applied Polymer Science

Melt rheological studies of polypropylene filled with coconut water treated and untreated fly ash

S. Radhakrishnan,[1] M. B. Kulkarni,[1] Nikesh Samarth,[2] P. A. Mahanwar[2]
[1]Maharashtra Institute of Technology, Kothrud, Pune, Maharashtra 411038, India
[2]Institute of Chemical Technology, Matunga, Mumbai, Maharashtra 400019, India
Correspondence to: S. Radhakrishnan (E-mail: radhakrishnan.s@mitpune.edu.in)

ABSTRACT: The melt rheology of polypropylene (PP) filled with fly ash (FA) before and after treatment with coconut water (CW) was studied for different concentration of the filler. The fly ash after coconut water treatment clearly showed additional peaks in the infrared (IR) spectra corresponding to the hydroxyl and carbonyl groups indicating good adsorption of CW on FA. The X-ray diffraction of melt compounded PP filled with CW-treated (CWT) FA showed large reduction of the main silica peak of FA and considerable broadening of Mullite and hematite peaks suggesting formation of fine particles by this treatment. Scanning electron microscopy (SEM) confirmed the drastic reduction of particle size in these composites. The melt rheological studies for these composites indicated considerable increase in viscosity at low filler loading for CW treated FA. The concentration dependence of melt viscosity did not follow any of the theoretical equations suggested in literature. Although, the behavior was similar to nanoparticle-filled polymers, there were some differences especially above the critical concentration of 4.5% by volume. The frequency dependence of storage and loss modulus indicated crossover point clearly, which was greatly affected by CW treatment. The Cole–Cole plots of real and imaginary part of melt viscosity brought out the broad distribution of relaxation time for the CW treated FA. The CW treated FA melt compounded with PP gave rise to nanocomposites with uniform dispersion. However, above 4.5% by volume, there appears to be agglomerate formation along with a thin interfacial layer, which assists the melt flow even at high filler loading. © 2016 Wiley Periodicals, Inc. J. Appl. Polym. Sci. **2016**, *133*, 43900.

KEYWORDS: composites; nanoparticles; nanowires and nanocrystals; polyolefins; synthesis and processing; viscosity and viscoelasticity

Received 2 January 2016; accepted 29 April 2016
DOI: 10.1002/app.43900

INTRODUCTION

Polypropylene (PP) has been extensively studied and used for large number of applications. It has been mostly used in filled form with variety of fillers ranging from calcium carbonate, talc, mica, glass fibers, natural fibers, nanoclay, etc.[1–5] Various properties have been studied and these have been correlated with supermolecular structure, interaction with fillers, additives, etc.[6–10] Amongst the different types of fillers, fly ash (FA) is an attractive option since it is easily available, cost effective, and it can improve properties such as thermal stability, wear resistance, flexural strength, etc.[11–14] Fly ash has been studied as a filler in number of polymer matrices such as epoxy, poly(vinyl chloride), polyethylene, poly(ether ether ketone), etc.[15–17] In polyolefins such as high-density polyethylene (HDPE) or polypropylene (PP), there is a need to incorporate surface treatment/compatibilizer to improve the properties of FA composites. It is essential to know the melt flow behavior of polymers filled with fly ash since this leads to better processing conditions for consistent product properties. There are very few reports on the rheological behavior of fly ash filled polymer especially polypropylene. Further, amongst the treating agents used for fly ash, no report is available on natural product such as coconut water (CW) as treatment agent. Coconut water (CW), which again often goes waste, is an interesting natural product with many chemicals such as polyols, proteins, sugars, and long chain carboxylic compounds, which bind metal ions.[18] CW has been used even for generation of nanoparticles of $NiFe_2O_4$.[19] Further, fly ash is known to be porous and it can adsorb easily many liquids, coupling agents, etc.[20] The treatment of FA with CW was taken up not for dispersing the filler but for size reduction. It may be pointed out that recently it has been reported that coconut milk when heated to 150–160 °C

Additional Supporting Information may be found in the online version of this article.

leads to formation of carbon quantum dots with size of few nm.[21] It has also been reported that nano particles of silver can be generated with the use of coconut water.[22] The control of particle size of Y_2O_3:Eu^{3+} with coconut water assisted sol-gel process has also been reported.[23] The polar groups of the chemicals present in CW can attach to the metal oxides presenting FA. Further, FA has high porosity in which CW can get absorbed. FA also has catalytic activity, which may lead to production of carbon nano particles. In our experiments, the CW-treated (CWT) FA after melt compounding with PP at 220 °C led to the formation of particles of size < 200 nm. This can affect the viscoelastic properties of the melt as well as the composite. It is conjectured that CW treatment of fly ash may generate new structures, better coupling between FA and PP as well as lead to development of cost effective composites using waste materials. In this article, we report the melt flow behavior of PP filled with CW treated and untreated (UT) fly ash.

EXPERIMENTAL

Materials

Polypropylene (PP) used was supplied by Reliance Industries Ltd. (grade REPOL H110MA, MFI 11 g/10 min, and density 0.95 g/cc). The fly ash (FA) was cenosphere type supplied by Envirotech Engineers, Pune, India having average particles of 150 mesh sieve size. Coconut water (from tender green coconut) was purchased from local supplier. More details on composition are given in the Supporting Information provided for this article.

Surface Treatment of Fly Ash

Experiment was performed by taking 1:2 ratios of fly ash to coconut water respectively. Before treatment of fly ash with coconut water, the coconut water was filtered thoroughly. About 250 g of fly ash was treated in 500 mL coconut water and was completely soaked for 24 h. The coconut water was taken in a container and the FA (about 50% wt/wt) is added step-by-step with continuous stirring. The treatment is performed for 24 h under continuous stirring. The treated fly ash was then dried at 80–85 °C for 3 h. After drying, the treated fly ash increased in weight due to the residual solids getting deposited from CW, which was 0.5 to 0.75% wt/wt of FA.

Preparation of Compositions

The compounding of PP with various concentrations of 0, 10 20, 30, and 40 weight percent of the untreated and treated fly ash filler were carried out using twin screw extruder (M/s APV Baker, UK, and Model: MP19PC). In this process, the temperature profiles in the barrel were: Zone 1: 170 °C, Zone 2: 190 °C, Zone 3: 200 °C, and Zone 4, 210 °C; die temperature, 220 °C; and the screw rotation rate of 60 rpm was used and then extruded strands were then pelletized. The volume percentage in the final product was determined using the standard formula with PP density of 0.95 g/cc and FA density of 2.36 g/cc since the particle size and morphology changed after melt processing, especially after treatment as explained later in this article. All compositions studied in present work are summarized in Table I.

Table I. Different Compositions of PP-FA Studied

Sr.	Polymer PP Repol H110MA (vol %)[a]	Filler fly ash (vol %) with and without CW treatment
1	100	0
2	95.5	4.5
3	90.3	9.7
4	84.5	15.5
5	78.0	22.0

[a] Volume % estimated from the weights and densities of the polymer and filler.

Characterization

The synthesized samples along with raw material were analyzed using Fourier transform infrared (FTIR) spectrometer (model Alpha diamond ATR Bruker). The single bounce attenuated total reflection (ATR) mode was used to obtain the infrared (IR) spectra of the treated and untreated FA samples to study the surface modification due to treatment. The structural changes of the prepared composites were determined by X-ray diffraction (XRD) analysis using (model Rigaku) unit fitted with miniflex goniometer. The normal focus copper X-ray tube was operated at 30 kV and 15 mA. Samples were in the form of molded discs and diffraction pattern was recorded in the 2θ range of 5.00° to 60.00° at the scan rate of 3.00°/min. The data processing was done using Jade 6.0 software. The field emission scanning electron microscopy (FE-SEM) was carried out on fractured injection molded samples after coating the surface with conducting layer. FE-SEM (Model JSM 6360 JEOL, Japan) was used for recording the images. Transmission electron microscopy (TEM) was carried out using microscope (model 1200ES JEOL Japan).

Rheological Studies

The melt viscosity was measured using rotational rheometer (MCR101, Anton Paar, India) with parallel plate assembly having diameter of 35 mm. Samples were pre-dried before analysis. Viscosity was determined for shear rates from 0.01 s^{-1} to 100 s^{-1} at the constant temperature of 250 °C. The storage and loss modulus values were directly obtained from the instrument. The melt viscosity was measured using rotational rheometer (model MCR101, Anton Paar, India) with parallel plate assembly having diameter of 35 mm. Samples were pre-dried before analysis. Viscosity was determined for different angular frequencies ranging from 0.01 rad s^{-1} to 100 rad s^{-1} at the constant temperature of 250 °C.

RESULTS AND DISCUSSION

Characterization (for More Details see Supporting Information)

The modification by treatment of FA with coconut water was clearly seen from the FTIR and XRD. Figure 1 shows the FTIR spectra of treated and untreated FA after drying. The few peaks of FA noted in the range of 1,200 cm^{-1} to 500 cm^{-1} are assigned to silica and alumina.[24] The band at 1,082 is due to Si—O—Si stretching, 783 cm^{-1} is due to Al—O vibration mode,

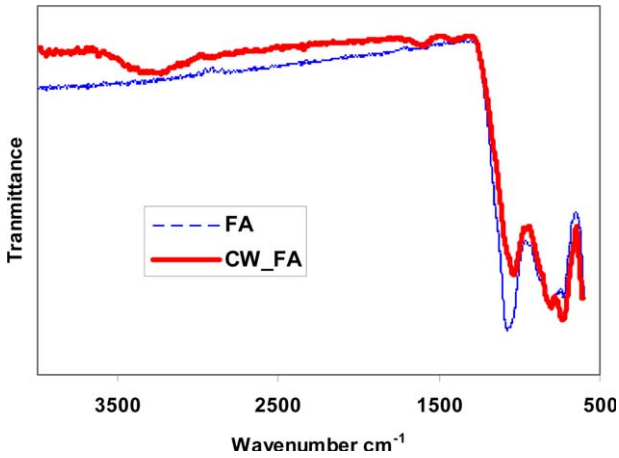

Figure 1. FTIR spectra of fly ash with (CW FA) and without treatment (FA) by coconut water. [Color figure can be viewed in the online issue, which is available at wileyonlinelibrary.com.]

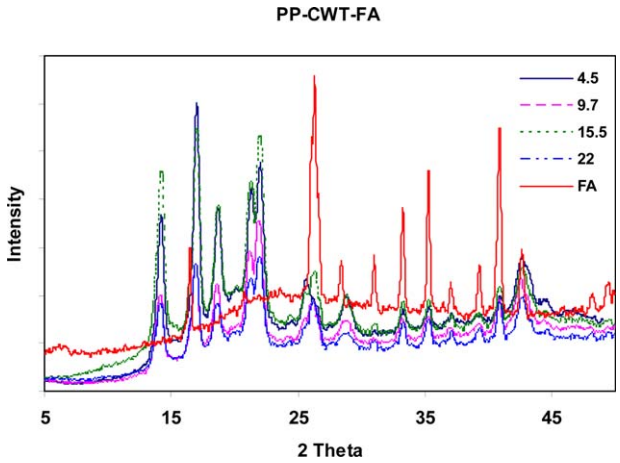

Figure 2. XRD scans for PP melt compounded with CW treated FA. The numbers correspond to vol % FA. The XRD for untreated FA powder is shown for comparison. [Color figure can be viewed in the online issue, which is available at wileyonlinelibrary.com.]

and 600 cm^{-1} is due to Si—O—Al stretching. However, CW treated FA samples exhibit clearly new bands at 3,300 cm^{-1} (broad), 1,566 cm^{-1}, and 1,368 cm^{-1}, which are due to Si—OH group and —OH group, respectively. The relative intensities of the peaks at 1,050, 790, and 705 cm^{-1} are also clearly seen to change after CW treatment. These observations clearly indicate that CW is adsorbed to the FA particles bringing about surface modification. The XRD of PP with untreated and CW treated FA is indicated in Figure 2. For comparison, the XRD of FA alone is also indicated. It is evident that there are many peaks of FA, which reduce in intensity in the PP composite. In particular, the major peak of FA at 26.35°, which is due to quartz form of silica, decreases considerably in the PP matrix after melt processing. This reduction together with its broadening is more in the case of CW treated FA. The number of peaks in FA can be assigned to Mullite (-aluminum silicate), quartz/silica, iron oxide, calcium oxide, and calcite. Amongst these, the

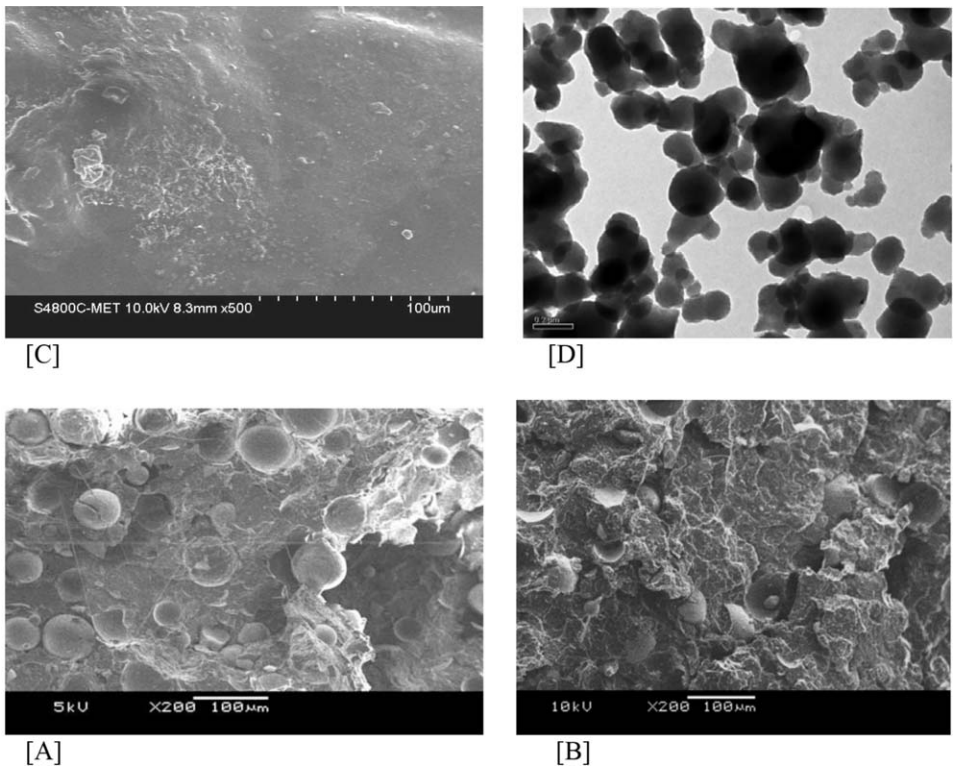

Figure 3. FE-SEM and TEM photographs depicting change in FA particle size: (A) PP-FA, (B) PP-FA with titanate coupling agent taken from Ref. 14, (C) PP-FA with CW treatment after melt compounding. (D) shows the TEM of PP with CW treated FA melt compounded pellet after dissolving in hot xylene and casting a drop on TEM grid. The scale bar in TEM is 0.2 micron.

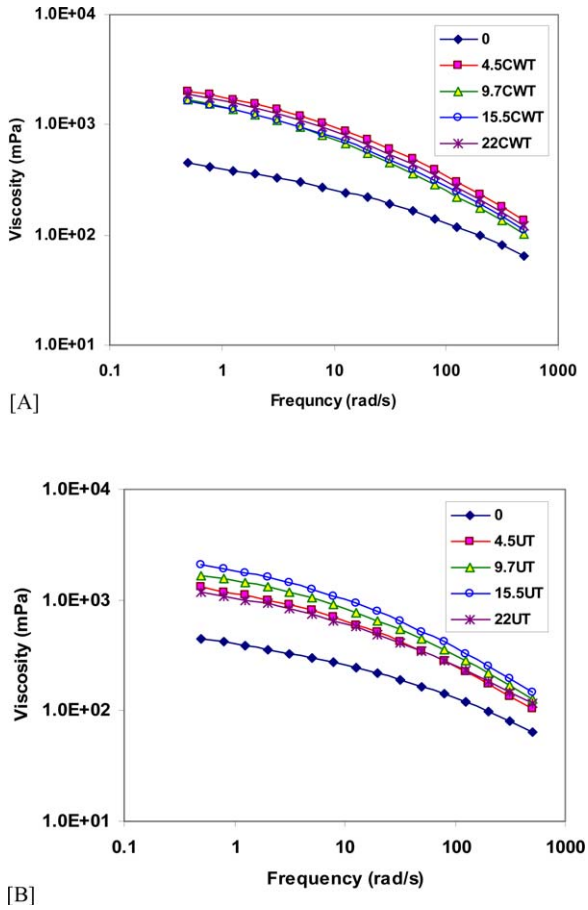

Figure 4. Complex viscosity of PP-FA (A) with CW treatment and (B) without treatment. The numbers for the legends indicate the vol.% of the FA. Melt temperature was 220 °C. [Color figure can be viewed in the online issue, which is available at wileyonlinelibrary.com.]

quartz peak is the most prominent followed by Mullite and then iron oxide. It is interesting to note that the iron oxide peak at 33.1° becomes prominent but quite broad in the composite while Mullite peaks are decreased and broadened considerably. A few authors have attempted to make nano particulate fly ash by high-energy ball milling.[25,26] They also report reduction of the main quartz peak at 26.35° along with its broadening and attribute the same to size reduction of FA particles. However, the reduction in their case is much less than the present case. In their case, the reduction after 60 h ball milling is up to 0.47 of its original while in the present case after CW treatment and melt compounding with PP, this peak intensity reduces to 0.3 of its original. Thus, it appears that the shearing action during melt compounding of the PP-CWTFA composites leads to better reduction in FA particle size as the CW embedded inside the FA suddenly outbursts. The CW treatment helps this process since the polar groups attach to FA surface and non-polar tail gets pulled by PP melt. The surface of FA gets broken and shattering of particles takes place by internal movement of organic components embedded in the FA cenospheres during melt compounding with PP. The peaks occurring at 14.2, 16.9, 18.7, 21.3, and 21.9 belong to the (110), (040), (130), (140), and (111) reflections from alpha form of PP.[27] There are some changes in the relative intensities of these peaks but PP remains only in alpha form after the addition of untreated and CW treated FA. Further evidence for shattering of FA particles due to coconut water treatment and melt processing is obtained from the FE-SEM studies as well as TEM images. Figure 3 shows the micrographs of fractured samples of FA in PP: (A) the untreated, (B) treated with titanate coupling agent (from Ref. 14), and (C) coconut water treated. It is quite evident that CW treatment prior to melt processing leads to shattering of the FA particles and resulting fragments which are in the submicron range. The TEM image shown in Figure 3(D) indicates that the particles are less than 0.2 micron or 200 nm. It should be mentioned here that the scanning electron microscopy (SEM) of samples containing high concentration of CW–FA reveals agglomerate formation clearly. These various aspects have been described in detail in the Supporting Information of this article.

Rheological Studies. The complex viscosity as a function of shear rate for PP with different concentrations of untreated (UT) FA and CW treated (CWT) FA is shown in Figure 4(A,B) respectively. It is seen that there is a gradual increase of viscosity with the increase of addition of UT FA while the increase is rapid for CWT FA. In call cases, the shear thinning behavior is observed just as in PP but the transition between Newtonian to non-Newtonian one becomes more evident in the filled systems than PP itself. The concentration dependence of melt viscosity at low shear rate (0.5/s) for these two cases is shown in Figure 5. It is evident that there is a sudden rise in viscosity even at low concentration (4.5% by volume) of CWT FA and it

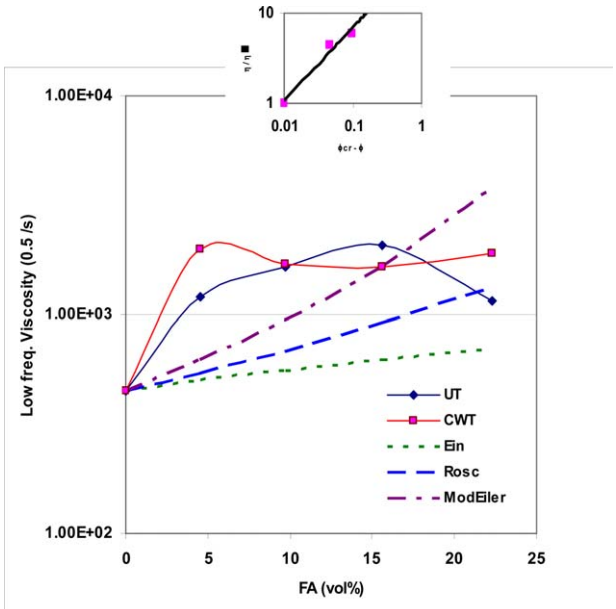

Figure 5. Low frequency (0.5/s) viscosity with respect to concentration of FA with and without CW treatment. The dotted curves represent the variation as per the models. The inset shows the log–log plot for percolation type relation. [Color figure can be viewed in the online issue, which is available at wileyonlinelibrary.com.]

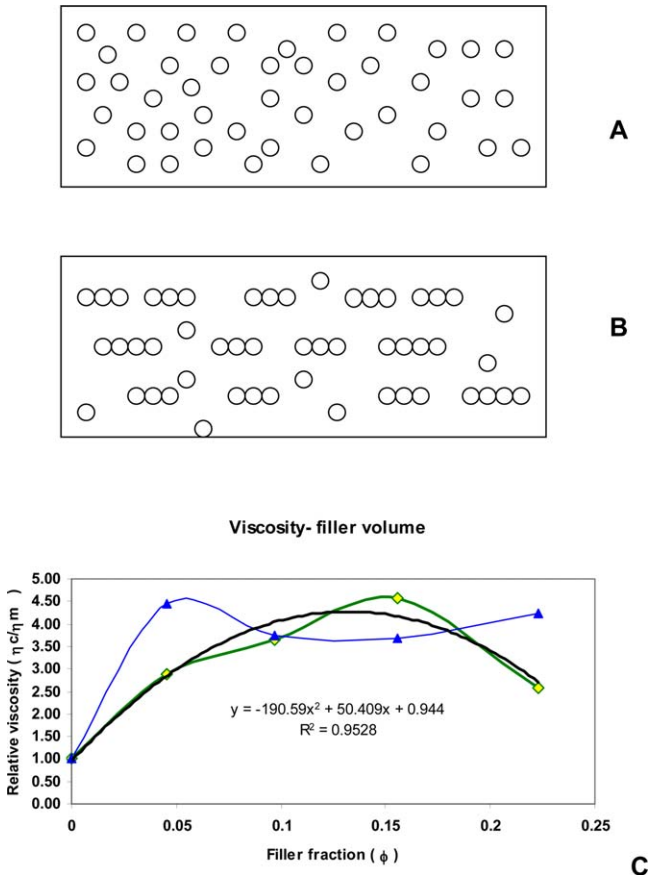

Figure 6. Schematic representation of possible particle agglomeration and redistribution in PP containing CW treated FA. (A) at low concentration and (B) at high concentration (> critical concentration). The polynomial fit to the untreated FA containing PP is good but CW treated FA in PP behaves differently. [Color figure can be viewed in the online issue, which is available at wileyonlinelibrary.com.]

continues to remain high for other concentrations. However, for UT FA, the increase of viscosity is more gradual up to a concentration of 15% by volume, but it decreases beyond this for higher concentration. The addition of fillers to polymer solution or melt is known to increase the viscosity and there are number of theoretical models suggested to explain the same.[28–30] Amongst these models giving different relationships between viscosity (η) and volume fraction (Φ) of the filler, Einstein, Mooney, Roscope, and modified Eiler's equations are well known. These are given as

Einstein's equation

$$\eta_c = \eta_p(1+K_E\Phi) \quad (1)$$

where K_E is Einstein coefficient mostly = 2.5.

Mooney's equation

$$\ln\left(\eta_c/\eta_p\right) = (K_E\Phi)/(1-\Phi/\Phi m) \quad (2)$$

where Φm is the maximum filler volume fraction for a given packing geometry and aspect ratio of the filler. It is 0.632 for spherical particles randomly distributed.

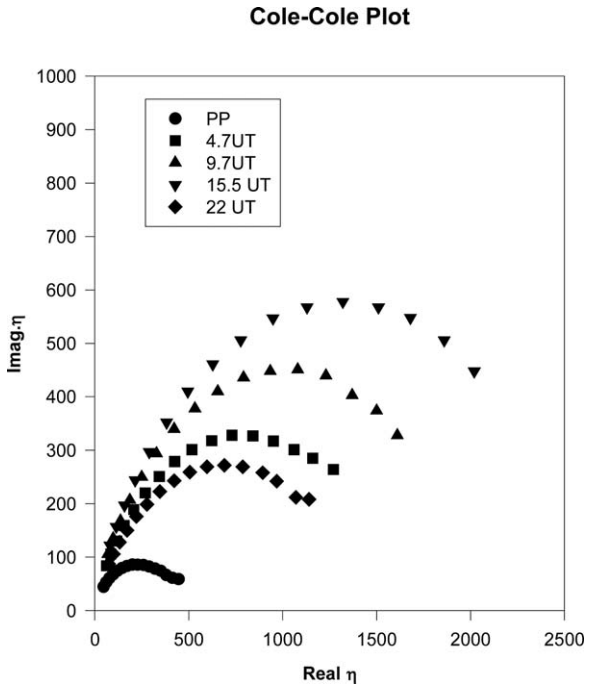

Figure 7. Cole–Cole plot for PP containing untreated FA.

Roscope (modified) equation

$$\left(\eta_c/\eta_p\right) = (1-\Phi/\Phi m)^{-2.5} \quad (3)$$

Modified Eilers–van Dijck relation

$$\left(\eta_c/\eta_p\right) = [1+(1.25\ \Phi/\Phi m)/(1-\Phi/\Phi m)]^2 \quad (4)$$

where Φm changes with agglomeration of the nano particles and it can be 0.37. In all the above equations, the subscript p

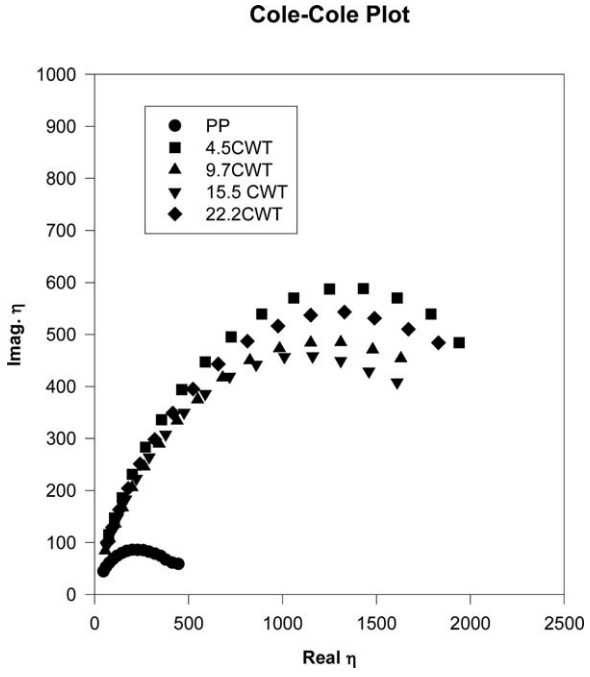

Figure 8. Cole–Cole plot for PP with CW treated FA.

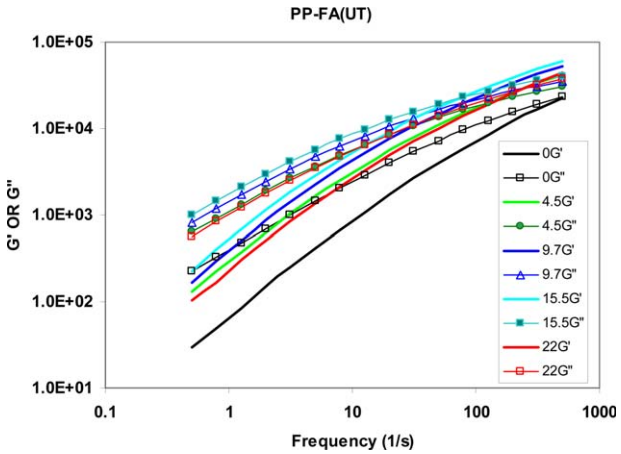

Figure 9. Storage and loss modulus for PP-FA without treatment as function of angular frequency. [Color figure can be viewed in the online issue, which is available at wileyonlinelibrary.com.]

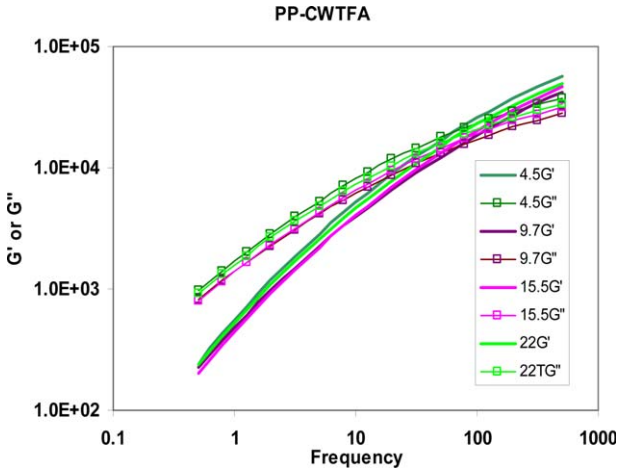

Figure 10. Storage and loss modulus for PP-FA with CW treatment as function of angular frequency. [Color figure can be viewed in the online issue, which is available at wileyonlinelibrary.com.]

and c refer to polymer and composite (filled) melts, respectively.

Figure 5 depicts these relations as dotted lines for comparison with the experimental data. None of these equations are apparently followed in the present case. Considering the fact that CWT treatment leads to formation of nano-particulate FA, which has been discussed earlier in the article, one may have to

Table II. Crossover Points for Untreated and Treated FA + PP

	UT		CWT	
Conc.	Fcr	G′=G″	Fcr	G′=G″
0	500	2.35E+04	500	2.35E+04
10	126	2.10E+04	79.2	2.24E+04
20	79.2	1.98E+04	79.2	1.63E+04
30	79.2	2.30E+04	79.2	1.77E+04
40	199	2.54E+04	79.2	1.99E+04

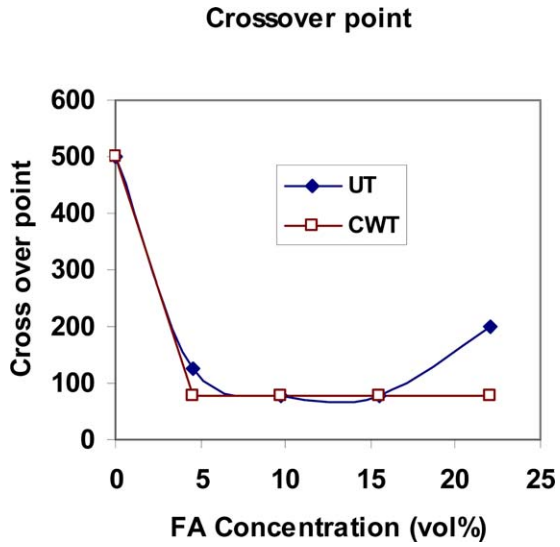

Figure 11. Variation of crossover point with FA concentration for untreated and CW treated cases. [Color figure can be viewed in the online issue, which is available at wileyonlinelibrary.com.]

consider the percolation type equations for viscosity as well.[31,32] For the nano particles dispersed in polymer matrix, the viscosity is given by the well-known percolation type equation

$$\left(\eta_c/\eta_p\right) = (\Phi - \Phi_{cr})^a \text{ for } \Phi > \Phi cr \quad (5)$$

$$\left(\eta_c/\eta_p\right) = (\Phi_{cr} - \Phi)^b \text{ for } \Phi < \Phi cr \quad (6)$$

where a and b are exponents and Φ_{cr} is the critical concentration or percolation threshold.

In the present case, the exponent was estimated from log–log plot and it is 0.67 while the threshold Φ_{cr} is 0.01, which fit the data for CWT FA as indicated in the inset of Figure 5. Although the initial part just near the percolation transition is reached appears to follow the power law as depicted in equation above, the trend seen at higher concentration of CW treated FA is quite different from those reported for nanoparticle dispersed polymer melts. There are some reports which clearly state that the viscosity decreases after the addition of nanoparticles.[33,34] Especially for nano-silica, the drop in viscosity is quite prominent. Jain *et al.*[35] reported a drop of almost one order in melt viscosity at 5 wt % of nano silica in PP melt. They had synthesized nano-particulate silica within porous PP. In our case, CW treated FA forms nano particles, which are predominantly silica and Mullite are also synthesized during melt processing. It thus appears in the present case, that both processes of increase as well as decrease of viscosity are taking place. The former is in the initial stage while at higher concentration the latter process is also taking place simultaneously leading to an upper limit to the viscosity. The decrease of the viscosity at higher concentration of the filler can be due to agglomerate network formation, as depicted schematically in Figure 6, which effectively reduces the polymer-filler contact surface area and/or formation of slip layer which allows the melt to flow easily under shear. It may be pointed out here that, the untreated FA particles do not show rapid rise in melt viscosity; there is a gradual increase up

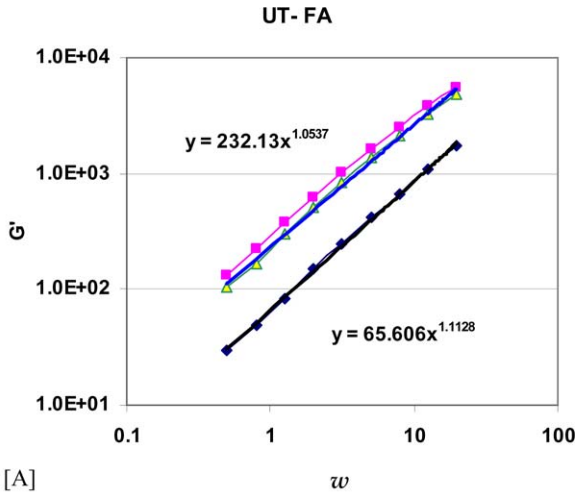

Figure 12. Frequency dependence of G′ on log–log scale depicting the square law (theory) and actual exponent with closest fit. (A) for untreated FA with lower curve for PP alone and (B) is for CW treated FA in PP and lower curve depicting square law. [Color figure can be viewed in the online issue, which is available at wileyonlinelibrary.com.]

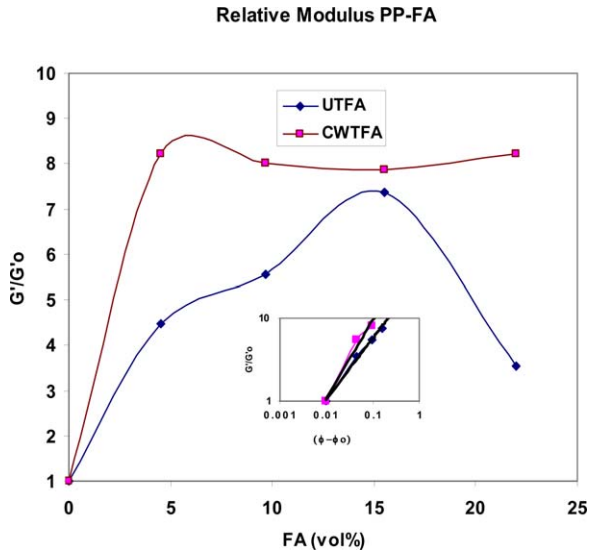

Figure 13. Relative modulus with respect to filler concentration in PP-FA system with and without CW treatment. The inset shows the log–log curve for low concentration of filler depicting percolation type behavior. [Color figure can be viewed in the online issue, which is available at wileyonlinelibrary.com.]

to 16 vol % above which there is a drop in viscosity. The data can be fitted with second order polynomial of the type

$$(\eta/\eta_o) = 1 + A\,\Phi + B\,\Phi^2 \qquad (7)$$

where A and B are coefficients determined from fitting equation, which are here 50.4 and −190.5 with R^2 of 0.96, which is depicted in Figure 6(C). The above equation is similar to that suggested by Batchelor[36] with different coefficients, which is modification of Einstein's equation if A = 2.5 and B = 0. The polymer-filler interaction is seen to be more pronounced in the case CW treated FA as indicated from the Cole–Cole plots of real (η′) and imaginary (η) parts of the complex viscosity, which are depicted in Figures 7 and 8. It is seen from these plots that the pure PP has almost semicircular plots with little breadth, whereas the graphs become the pure PP has almost semicircular plot with little breadth, the graphs become increasingly broader and skewed with increase of FA concentration. This tendency is more pronounced for CW treated FA. This type of trend has been reported in a number of polymers containing nano particles.[37–40] It may be mentioned that for heterogeneous systems containing networks, the elastic component increases together with higher relaxation time. Above the percolation threshold, the nanoparticles are known to form network like structures and finally agglomerates. This may be the reason for the increasing broadening of the Cole–Cole plots.

The storage and loss modulus (G′ and G″) were determined from the rheometer for all these compositions. Figure 9 show the plot of G′ and G″ with radial frequency for PP and PP filled with untreated FA while Figure 10 shows the similar graphs for PP filled with CW treated FA. In both these figures, it is seen that the curves for G′, which are much below the G″ curves at lower frequencies cross over and go to higher values above the G″. The cross over is quite evident in the filled PP and more,

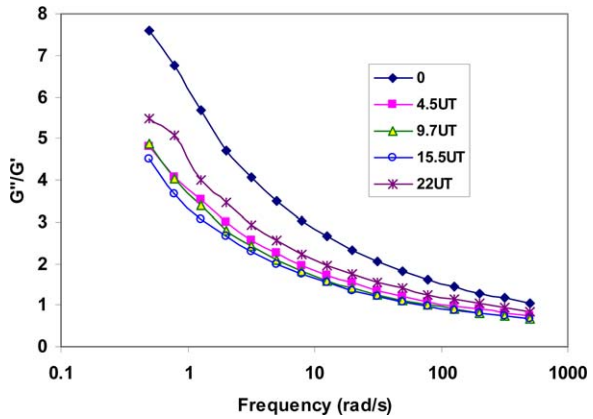

Figure 14. Damping factor tan δ (G″/G′) with frequency for PP containing untreated FA. The numbers next to legends indicate the % by volume of FA. [Color figure can be viewed in the online issue, which is available at wileyonlinelibrary.com.]

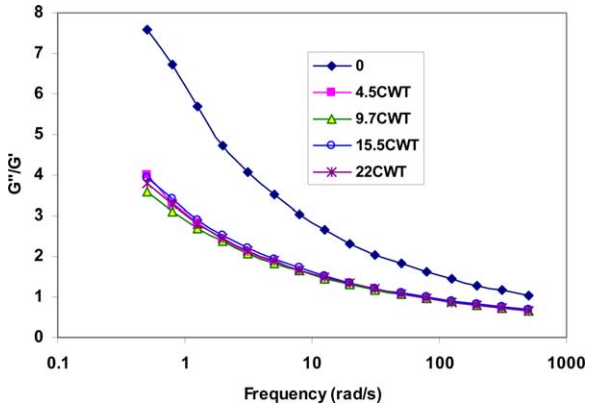

Figure 15. Damping factor tan δ (G″/G′) with frequency for PP containing CW treated FA. The numbers next to legends indicate the % by volume of FA. [Color figure can be viewed in the online issue, which is available at wileyonlinelibrary.com.]

so for CW treated FA. However, PP by itself does not exhibit clear cross over in the frequency region studied; the G′ and G″ for pure PP tend to only merge at high frequencies. The cross over point for the G′ and G″ is well reported for polymers containing fillers and fibres.[40,41] It indicates the change of viscoelastic behavior of the dispersion: going from flowing melt to semi-solid like behavior.[42] Table II gives the values of the crossover point and the values for G′=G″ for different concentrations of the FA. The trend of cross over point with FA concentration is indicated in Figure 11. It is interesting to see that for CW treated FA, the crossover takes place at much lower frequency and after that there is little change. However, for untreated FA, there is first shift to lower frequency while at higher loading of the filler, the crossover shifts back to higher frequency suggesting agglomeration of the particles.

The frequency dependence of G′, in the low regions in polymers, is given by some authors as $G' \alpha w^2$.[40] However, in the present case, G′ depends as $w^{1.12}$ for pure PP and it progressively changes to $w^{0.9}$ with the increase of FA content for untreated case. Figure 12 shows the comparison of the experimental data with power law fit and the square law ideal curve. The lower curve in Figure 12(A) is for PP alone while the upper is with untreated FA. However, the exponent is still lower for CW treated FA in PP wherein $G' \alpha w^{0.78}$ which is seen in Figure 12(B). The change in the characteristic terminal behavior can be attributed to the filler-polymer interaction leading to more solid elastic type relaxation than viscous melt like response. The transition or cross over point discussed above also confirms the same. It is interesting to note that although CW treated FA gives some effects similar to those documented in other cases such as nano-clay filled HDPE, nano-silica filled PP, acrylic polymer filled with nano-whiskers and others.[37–39] However, there are quite a few differences in the expected behavior than that for nano particle filled polymers. In the nano-particulate filled polymers, the concentration dependence of G′ is expected to follow $G' \alpha A\Phi^m$ type relation.[37] Figure 13 shows the concentration dependence of G′ for untreated and CW treated FA in PP. In the case of untreated FA, there is a gradual increase of G′ up to the volume concentration of 16% above which it drops to some extent which could be due to agglomeration and possible phase separation. However, for the CW treated FA, there is sudden increase of G′ even at low concentration of 4% by volume and it continues to be high above this concentration suggesting that upper value is attained. These findings suggest that the CW treated FA forms a network up to 9.5% by volume above which there are only aggregate formation and hence the additional filler does not disperse in the nano form. Thus, there is an upper limit for the particles to be dispersed uniformly in melt processing of PP with CW treated FA. Since, at higher concentrations, there is aggregation, the interaction with the polymer melt is reduced and the viscosity is affected to only small extent.

The loss factor tan δ (G″/G′) which is related to energy dissipation in the medium for the untreated and treated FA in polypropylene is shown in Figures 14 and 15, respectively. It is interesting to note that the loss factor is high at low frequency and decreases with the increase of frequency but there is no distinct peak observed in the range of frequencies studied. There is a small indication that there can be a peak for untreated FA at 22% by volume loading occurring at 0.5 rad s^{-1}. It may be observed that for untreated FA, the loss factor first reduces and then again increases with the increase of FA concentration. However, for CW treated FA the loss factor decreases and remains low at all concentrations. This again suggests that for CW treated FA the matrix becomes quite stiff while in the case of untreated FA, the matrix is more pliable.[43,44]

CONCLUSIONS

The present studies on fly ash filled polypropylene with and without treatment show that treatment by coconut water prior to compounding is quite effective in reducing the fly ash particle size. This process can generate nanosized fly ash which can be well dispersed in polypropylene. The rheological behavior of the treated FA in PP resembles very much the nano particle dispersed polymer melts with large distribution of relaxation time, increase in the storage modulus and sudden rise in complex viscosity. Also, the crossover point of G′ and G″ is distinctly seen in these systems which indicates the change over from viscoelastic to elastic behavior. These studies suggest that coconut water can be effective not only for generating sub-micron particles of FA but also for increasing the particle-matrix interaction.

ACKNOWLEDGMENTS

Authors wish to thank V. D. Karad, Founder President MAEER's, Maharashtra Institute of Technology, Pune for his constant encouragement and support during the project. They also wish to thank Director, ICT, Mumbai for extending the facilities for carrying out some of the experiments.

REFERENCES

1. Pukanszky, B. In Polypropylene: Structure Blends and Composites; Karger-Kocsis, J., Ed.; Chapman & Hall: London, **1995**; p 142.
2. Karger, K. J. *Polym. Compos.* **2000**, 21.

3. Zhao, R.; Huang, J.; Sun, B.; Dai, G. *J. Appl. Polym. Sci.* **2001**, *82*, 2719.
4. Lukas, S.; Reinhold, W. L.; Andreas, H. *Compos. Sci. Tech.* **2012**, *7*, 550.
5. Ciardelli, F.; Coiai, S.; Passaglia, E.; Pucci, A.; Ruggeri, G. *Polymer Int.* **2008**, *57*, 805.
6. Pukanszky, B. Polypropylene An A–Z Reference; Karger-Kocsis, J., Ed.; Kluwer Academic Publisher: Dordrecht, **1999**; p 240.
7. Saujanya, C.; Radhakrishnan, S. *Polymer* **2001**, *42*, 6723.
8. Shubhra, Q. T. T.; Alam, A. K. M. M.; Quaiyyum, M. A. *J. Thermoplast. Compos. Mater.* **2011**, *26*, 362.
9. Hasegawa, N.; Okamoto, H.; Kato, A.; Uauki, M. *J. Appl. Polym. Sci.* **2000**, *78*, 1918.
10. Saujanya, C.; Radhakrishnan, S. *Polym. Compos.* **2001**, *22*, 232.
11. Barbuta, M.; Taranu, N.; Harja, M. *Environ. Eng. Magmt. J.* **2009**, *8*, 1145.
12. Ahmaruzzaman, A. *Prog. Energy Combust. Sci.* **2010**, *36*, 327.
13. Satapathy, S.; Nando, G. B.; Nag, A.; Raju, K. V. S. N. *J. Appl. Polym. Sci.* **2013**, *130*, 4558.
14. Kulkarni, M. B.; Mahanwar, P. A. J. *Thermoplast. Compos. Mater.* **2014**, DOI: 0892705713518795.
15. Kulkarni, M. B.; Mahanwar, P. A. *J. Thermoplast. Compos. Mater.* **2014**, *27*, 1679.
16. Atikler, U.; Basalp, D.; Tihminlioğlu, F. *J. Appl. Poly. Sci.* **2006**, *102*, 4460.
17. Parvaiz, M. R.; Mohanty, S.; Nayak, S. L.; Mahanwar, P. A. *J. Miner. Mater. Character. Eng.* **2010**, *9*, 25.
18. Prades, A.; Dronier, M.; Diop, N.; Pain, J. P. *Fruits* **2012**, *67*, 87.
19. De Paina, J. A.; Graca, M. P.; Oterio, J. M.; Macedo, M. A.; Valente, M. A. *J. Alloys Compd.* **2009**, *485*, 637.
20. Velado, D.; Potgieter, H.; Liauw, C. M. *J. Appl. Polym. Sci.* **2013**, *130*, 3985.
21. Roshni, V.; Ottoor, D. *J. Luminescence* **2015**, *161*, 117.
22. Elumalai, E. K.; Kayalivizhi, K.; Silvan, S. *J. Pharma Bioallied Sci.* **2014**, *6*, 241.
23. Gomes, M. A.; Valerio, M. E. G.; Macedo, Z. S. *J. Nanomaterials* **2011**, *2011*, 6.
24. Yilmaz, G. *J. Mole. Struct.* **2012**, *1019*, 37.
25. Thomas, P. K.; Satpathy, S. K.; Manna, I.; Chakraborty, K. K.; Nando, G. B. *Nanoscale Res. Lett.* **2007**, *2*, 397.
26. Patil, A. G.; Anandhan, S. *Int. J. Energy Eng.* **2012**, *2*, 57.
27. Cheng, S. Z. D.; Janimak, J. J.; Rodriguez, J. In Polypropylene Structure Blends and Composites, Karger Kocsis, J., Ed.; Chapman & Hall: London, **1995**; Vol. *1*, pp 31.
28. Mooney, M. *Colloid Sci.* **1951**, *6*, 162.
29. Roscoe, R. *Br. J. Appl. Phys.* **1952**, *3*, 267.
30. Barnes, H. A. In Rheology Reviews.; Binding, D. M.; Walters, K., Ed.; British Society of Rheology: UK, **2003**; pp 1–36.
31. Cassagnau, P. *Polymer* **2008**, *49*, 2183.
32. Dorigato, A.; Pegoretti, A.; Penati, A. *Express Polym. Lett.* **2010**, *4*, 115.
33. Goldansaz, H.; Goharpey, F.; Afshar-Taromi, F.; Kim, I.; Stadler, F. J.; van Ruymbeke, E.; Karimkhani, V. *Macromolecules* **2015**, *48*, 3368.
34. Wu, L.; Chen, P.; Chen, J.; Zhang, J.; He, J. *Polym. Eng. Sci.* **2007**, *47*, 757.
35. Jain, S.; Goosens, J. G. P.; Peters, G. W. M.; van Duin, M.; Lemstra, P. J. *Soft Matter* **2008**, *4*, 1848.
36. Batchelor, G. K. *J. Fluid Mechanics* **1977**, *83*, 97.
37. Cipriano, T. F.; Silva, A. L. N.; Silva, A. H. M.; Sousa, A. M. F.; Silva, G. M.; Nascimento, C. R. *J. Mater. Sci. Eng. B* **2013**, *11*, 695.
38. Abranyi, A.; Szazdi, I.; Pukanszki, B.; Vansco, G. J. *Macromol. Rapid Comm.* **2006**, *27*, 132.
39. Durmus, A.; Kasgoz, A.; Makosco, C. W. *Polymer* **2007**, *48*, 4492.
40. Jiang, L.; Zang, J.; Wolcott, M. P. *Polymer* **2007**, *48*, 7632.
41. Iyer, K. A.; Torkelson, J. M. *Polymer* **2015**, *68*, 147.
42. Du, F.; Scogna, R. C.; Zhou, W.; Brand, S.; Fischer, J. E.; Winey, K. I. *Macromolecules* **2004**, *37*, 9048.
43. Alkonis, J. J.; Macknight, W. J. Introduction to Viscoeleasticity; Wiley: New York, **1983**.
44. Malkin, A. Ya; Isayev, A. I. Rheology: Concepts, Methods and Applications; Chem Tech Publ.: Toronto, **1994**.